Performance Limitation and Mitigation of Longitudinal Spatial Hole Burning in High-Power Diode Lasers

Zhigang Chen*, Ling Bao, John Bai, Mike Grimshaw, Rob Martinsen, Mark DeVito, and Jim Haden
nLIGHT Corp., 5408 NE 88th Street, Bldg E, Vancouver, WA 98665

Paul Leisher
Department of Physics and Optical Engineering, Rose-Hulman Institute of Technology, Terre Haute, IN 47803

ABSTRACT

Facets of high-power broad area diode lasers are typically coated with one high-reflecting and one partially reflecting layer to improve slope efficiency and maximize output power. The typical cavity lengths of commercial devices have also been progressively increasing, mainly to reduce temperature rise at the active region and improve laser performance and reliability. The asymmetric reflectivities and long cavity length, however, result in a highly inhomogeneous longitudinal profile of the photon density, which induces a spatially non-uniform carrier distribution, so-called longitudinal spatial hole burning (LSHB). A more uniform longitudinal photon and carrier distribution is believed to improve the overall gain of the cavity and reduce gain saturation, although further study is required to understand the impact of LSHB to power efficiency and its implication in laser design optimization to achieve higher peak powers. We present a phenomenological model that incorporates LSHB to describe longitudinal photon and carrier density inhomogeneity, as well as light-current characteristics of a diode laser. The impact of LSHB on the power efficiency is demonstrated through numerical calculation and can be significant under high-power operations. This presents new guidelines for high-power diode laser designs, in which LSHB imposes limits on reducing facet reflectivity and/or increasing cavity length, beyond which performance deteriorates. Alternatively, effects of LSHB can be mitigated through longitudinal patterning of the waveguide or contact to achieve high-power and high-efficiency diode lasers. We propose specially designed longitudinal patterning of electrical contact to mitigate LSHB. Ongoing device implementation will be used to demonstrate performance benefits.

Keywords: longitudinal spatial hole burning, high-power diode lasers, tapered waveguide

1. MOTIVATION

The facets of high-power broad area laser diodes are typically coated with one high-reflecting (HR) and one partially reflecting (PR) layer to improve slope efficiency and maximize output power. On the other hand, the cavity length of high-power laser diodes has been getting progressively longer, mainly to reduce thermal resistance between the chip and heatsink, which mitigates temperature rise at the active region and improves diode performance and reliability. Both the asymmetric reflectivities and long cavity length, however, result in a highly inhomogeneous longitudinal profile of the photon density, which induces a spatially non-uniform carrier distribution within the laser cavity. Such spatial inhomogeneity, named longitudinal spatial hole burning (LSHB), has been studied theoretically [1] and measured experimentally [2,3]. For example, the longitudinal spatial inhomogeneity of carrier distribution has been measured using spontaneous emission through the n-side window [2] and from the side [3] of high-power laser diodes, where a higher carrier density is observed close to the HR than that to the PR facet for above-the-threshold current. The longitudinal inhomogeneity of photon and carrier density is believed to lead to output decrease due to gain saturation at high injection current [3,4,5], although some authors argued that it is an small effect [6]. Experimentally, a slightly flared laser with longitudinally varying emitter width was designed with the aim of reducing LSHB and improvement of peak output power [7,8]. Further study is however required to understand the impact of LSHB to power efficiency and its implication in laser design optimization to achieve higher peak powers. Here we present theoretical models that incorporate LSHB to describe longitudinal carrier and photon distributions, as well as light-current (L-I) characteristics of a diode laser. Further, numerical calculations reveal performance limitations on facet reflectivity and cavity length.

* zhigang.chen@nlight.net; phone 360.566.4460; http://www.nlight.net

2. MODELING AND SIMULATION

A phenomenological approach is commonly used to describe behaviors of diode lasers through a set of coupled rate equations related to the balances for carriers and photons [9]. The standard equations generally assume uniform longitudinal distribution of carrier and photon densities within the laser cavity. This is, however, not the case in high-power laser diodes, in which carrier and photon inhomogeneity is significant especially at high current. To incorporate the LSHB effect, one-dimensional rate equations for the carrier and photon densities are modified as [2,4]

$$\frac{dN}{dt} = \frac{\eta_i J}{qd} - \frac{N(z)}{\tau} - v_g g(z) N_p(z), \tag{1}$$

$$\frac{dN_p^{\pm}(z)}{dz} = \pm(\Gamma g(z) - \alpha_i) N_p^{\pm}(z), \tag{2}$$

with the boundary conditions of

$$N_p^+(0) = R_1 N_p^-(0), \tag{3}$$

and

$$N_p^+(L) = \frac{1}{R_2} N_p^-(L) \cdot \tag{4}$$

Here $N(z)$ is the local carrier density, and $N_p(z)$ is the local photon density, with $N_p = N_p^+ + N_p^-$, and N_p^+ and N_p^- denoting the forward and backward propagating photons, respectively. In the equations, η_i is defined as internal quantum efficiency, J as the current density which is assumed to be uniform, d as the active region thickness, τ as the carrier lifetime that includes spontaneous and nonradiative recombination in the device, v_g as the photon group velocity, Γg as the modal gain, and α_i as the intrinsic optical loss. Eq. (1) describes the change of carrier density through carrier injection and radiative and nonradiative recombination, and is set to be zero for steady state operation. The longitudinal photon inhomogeneity is depicted in Eq. (2) through local stimulated emission and intrinsic loss (spontaneous emission contribution to the photon density is generally assumed small and is therefore neglected), with the photon density variation depending on the propagation direction of the photons. To accommodate the spatial photon non-uniformity, the optical loss at diode facets (mirror loss) is treated as boundary conditions of photon densities at $z = 0$ (PR) and $z = L$ (HR), as shown in Eqs. (3) and (4), instead of the average mirror loss in the standard model. LSHB describes phenomenon of gain saturation under different longitudinal optical intensities. Specifically, the higher the local photon density, the larger the gain saturates, and the smaller the local carrier density. The gain saturation effect is automatically reflected in the last term of Eq. (1), $v_g g(z) N_p(z)$, in which an increased local photon density results in a decreased local gain, and vice versa, to maintain a constant value of the term. The general solutions to Eqs. (1) to (4) are shown to satisfy a threshold lasing condition of

$$\frac{1}{L}\int_0^L \Gamma g(z) = \alpha_i + \frac{1}{2L}\ln(\frac{1}{R_1 R_2}), \tag{5}$$

which evolves into the normal threshold condition if assuming a longitudinally uniform gain of $g(z)$.

To demonstrate the effect of LSHB on high-power laser diodes, we numerically solve the above carrier and photon rate equations through finite difference method. For comparison, the device parameters are chosen to represent one of nLIGHT's state-of-the-art 1470 nm InGaAsP quantum well laser diodes. The device geometry of our 1470-nm broad area diode laser consists of a 3.8 mm cavity length with a 150 μm strip width. The typical CW performance of the diodes includes a peak efficiency of ~ 39%, a threshold current of 1.7 A, and a slope efficiency of ~0.5 W/A. Material and device parameters used in the modeling are extracted from device characterization, or collected from published data. The material gain is approximated as a logarithmic function of carrier density. For modeling the thermal roll of L-I characteristics, we assume exponential dependence of the threshold current and slope efficiency on junction temperature, with exponential characteristic temperatures of T_0 and T_1, respectively. The voltage-current characteristics used in the model represent those from experimental data.

3. RESULTS AND DISCUSSION

Figure 1 shows the calculated results for the longitudinal profiles of the photon and carrier densities at several current levels under LSHB (solid line). For comparison, the spatial profiles without LSHB effect are also plotted (dashed line). The case for no LSHB is calculated by assuming constant gain/carrier density along longitudinal position z, but the spatial photon inhomogeneity described in Eq. (2) is allowed for better comparison with the case of LSHB. No thermal effect is considered at this point. Without LSHB, the carrier density is constant along z, while the optical intensity follows a near exponential dependence following Eq. (2). LSHB leads to strong decrease of carrier density and gain near the PR facet, accompanied by a rise near the HR facet. The optical intensity profile also deviates from the near-exponential due to gain saturation. The result is a photon density reduction near the PR facet, hence a lower output optical power. The spatial profiles of both the carrier and photon densities are uniform for currents below or equal to the threshold current (I_{th} = 1.7 A), but becomes more inhomogeneous with increasing current above threshold. This indicates that the effect of LSHB becomes significant especially for high current operation in high-power laser diodes.

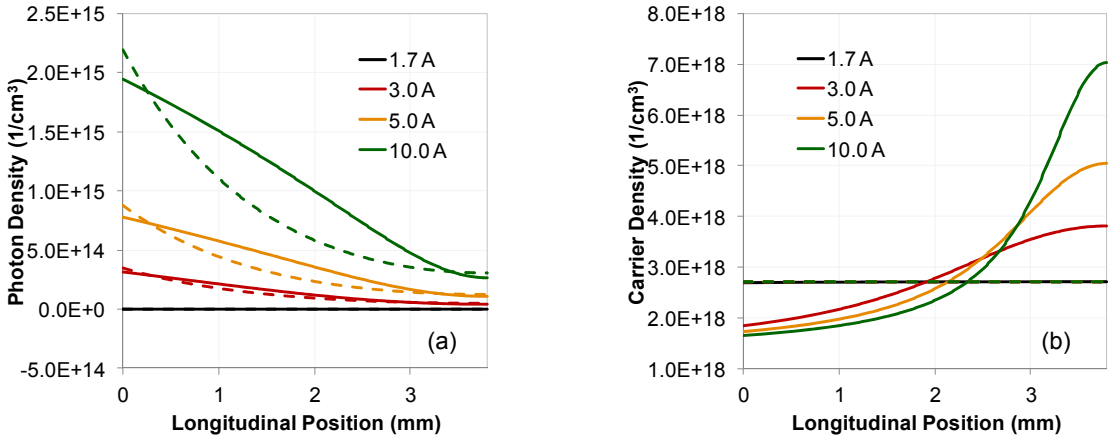

Figure 1. Calculated longitudinal profiles of (a) photon density and (b) carrier density at several above-the-threshold current. Solid lines: model with LSHB; dashed line: without LSHB. The PR and HR facets are at z = 0 and z = L, respectively. Thermal effect is not considered.

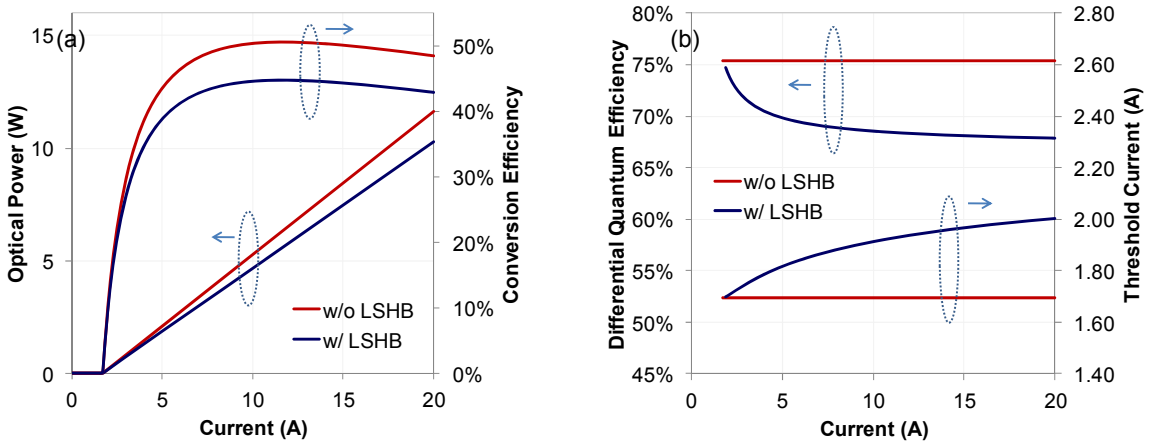

Figure 2. (a) Calculated L-I characteristics and conversion efficiency with and without considering LSHB effect. (b) DQE and threshold current as a function of injection current. Thermal effect is not considered.

The impact of LSHB to power efficiency of nLIGHT's 1470 nm laser diode can be revealed through the calculated L-I characteristics. Figure 2(a) shows the calculated optical power and conversion efficiency with and without including the LSHB effect. No thermal effect is considered at this point, representing experimental condition of QCW operation. Both the optical power and efficiency decrease when LSHB effect is included. Specifically, an 11% optical power decrease is calculated at an operating current of 10 A for the 1470 nm device. An alternative representation to the L-I curve is the current dependence of the differential quantum efficiency (DQE) and the threshold current, which provides additional information on the impact of LSHB to power efficiency. While the current dependent threshold current under LSHB is evaluated based on the longitudinal carrier density distribution using Eq. (1), the effective DQE can be calculated from the output power dependence on DQE and threshold current following

$$P = \eta_d \frac{\hbar\omega}{q}(I - I_{th}), \tag{6}$$

with η_d the DQE and I_{th} the threshold current. In the standard phenomenological approach,

$$\eta_d = \eta_i \alpha_m / (\alpha_i + \alpha_m), \tag{7}$$

with α_m the mirror loss. As shown in Figure 2(b), η_d under LSHB becomes progressively smaller at higher current as compared with that under no LSHB. This indicates a higher effective optical loss α_i with increasing current, as evident in Eq. (7). The increase of optical loss under LSHB is readily characterized through the longitudinal photon density distribution shown in Figure 1(a). As the current is increased, the photon density profile under LSHB deviates from the near exponential distribution under no LSHB, increasing the total number of photons stored in the cavity, hence higher optical loss of the laser diode. Similar arguments apply to the threshold current, where an asymmetric carrier density distribution results in higher spontaneous and nonradiative recombination rate, hence an increased threshold current. The increase of threshold current, however, has a smaller effect in limiting the output power under high current operation.

With the knowledge of current dependence of the threshold current and DQE under LSHB, the impact of temperature rise under CW operation can be readily described by phenomenologically imposing an additional exponential dependence of the threshold and DQE with the characteristic temperatures of T_0 and T_1, respectively. The calculated L-I characteristics, conversion efficiency, DQE and threshold are plotted in Figure 3 with and without including LSHB. As expected, because of the higher slope loss and threshold loss when LSHB effect is considered, the extra waste heat generated results in stronger thermal roll of the L-I characteristics. A 15% power reduction at a current of 10 A is observed under LSHB. The modeling parameters are optimized so that the calculated results under LSHB represents performance of nLIGHT's 1470 nm InGaAsP lasers, whose performance are plotted in Figure 3(a) as solids.

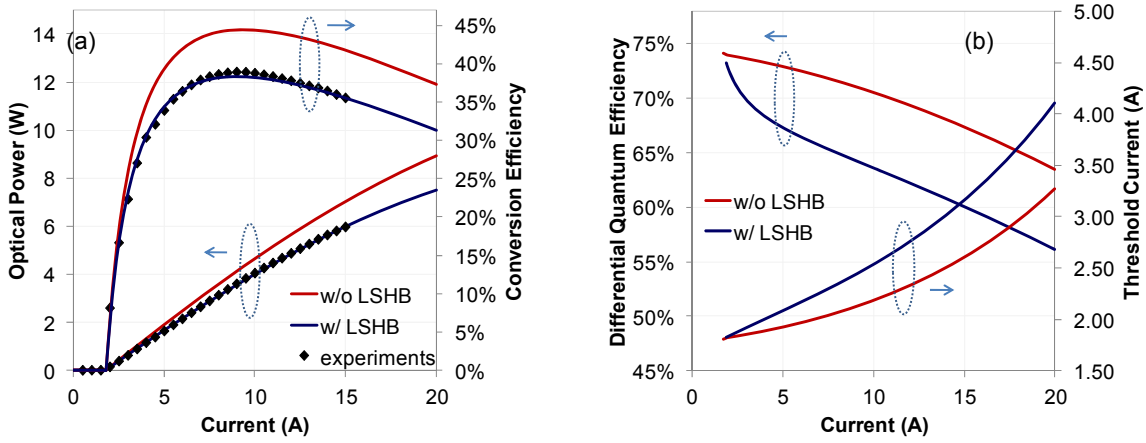

Figure 3. (a) Calculated L-I characteristics and conversion efficiency with and without considering LSHB effect. Solids: typical L-I and efficiency for nLIGHT's 1470 nm InGaAsP diode lasers. (b) DQE and threshold current as a function of injection current. Thermal effect is included by assuming exponential dependence of threshold current and slope efficiency on characteristic temperatures of T_0 and T_1, respectively.

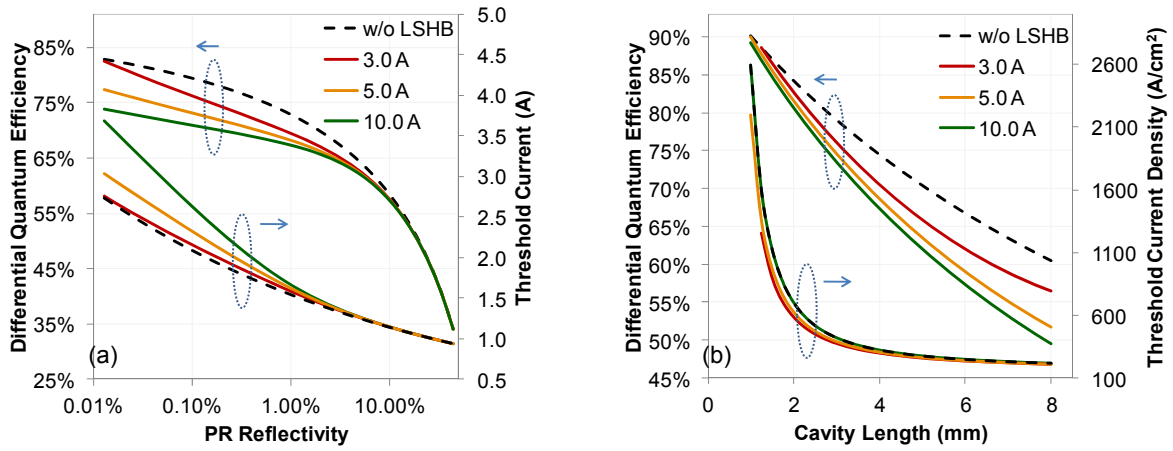

Figure 4. (a) Calculated DQE and threshold current as a function of PR reflectivity for several injection currents with LSHB (solid) and without LSHB (dashed). Cavity length of the laser is fixed at 3.8 mm. (b) Cavity length dependence for several injection currents with LSHB (solid) and without LSHB (dashed). The reflectivity of the PR is fixed at 0.5% for all cavity lengths. Thermal effect is not considered.

The PR facet of high-power laser diodes is usually coated with antireflection coating to improve the slope efficiency. Decrease of the PR reflectivity and the consequent increase of mirror loss results in an increased DQE. Such design criterion may not necessarily be proper when considering LSHB, as inhomogeneous optical intensity under LSHB affecting the DQE. We calculate the DQE and threshold current as a function of PR reflectivity for several injection currents with and without LSHB. The results are shown in Figure 4(a). The calculation assumes a fixed cavity length of 3.8 mm, which leads to increased DQE and threshold current with decreasing reflectivity for no LSHB (dashed line). When LSHB effect is included, the DQE and threshold current deviate from predictions from the standard model with reduced facet reflectivity, especially at high currents (solid line). Similar numerical results have also been presented in [3]. The smaller DQE and larger threshold current at low reflectivity indicates stronger LSHB effect under a more severe asymmetry of the PR and HR facet reflectivities. LSHB imposes a lower limit to the facet reflectivity, below which further reducing the reflectivity will not improve the slope efficiency and may deteriorate the overall performance of the laser.

Increasing the cavity length of high-power laser diodes has the advantage of mitigating temperature rise of the active region and reducing its effect on diode performance. Similar to the reflectivity dependence above, we calculate the dependence of DQE and threshold current *density* on cavity length. Because the reflectivities of the facets are fixed (PR at 0.5%), the standard model predicts that both the DQE and threshold current density decrease with increasing cavity length, shown as dashed lines in Figure 4(b). Under LSHB, the DQE decreases much quicker with increasing cavity length than that without LSHB, especially at high current. This suggests a more inhomogeneous photon density distribution at longer cavity length, and consequently larger optical loss under LSHB. The threshold current density, on the other hand, does not vary much with and without including LSHB effect. The simulation results show that LSHB imposes penalty on diode performance, which become greater with increased cavity length.

As described before, the root cause that limits the output power under LSHB is the increased optical loss due to the redistribution of photon density in the longitudinal direction. This indicates that a larger power penalty is expected in devices with higher intrinsic optical loss, α_i. This is indeed the case, confirmed by the calculated DQE and threshold current as a function of intrinsic optical loss in the cavity. As shown in Figure 5(a), the DQE deviation under LSHB effect becomes more severe when the intrinsic loss of the device is higher. In Figure 5(b), the percentage power reduction due to LSHB effect is calculated for several injection currents. A close to 20% power reduction is predicted for an intrinsic loss of 4 cm^{-1}, as compared with about 7% for 1 cm^{-1}. The performance penalties imposed by LSHB is shown to become more severe in devices with higher intrinsic loss. This also indicates that mitigating the LSHB effect will enhance power and efficiency performance, especially in devices with high optical loss.

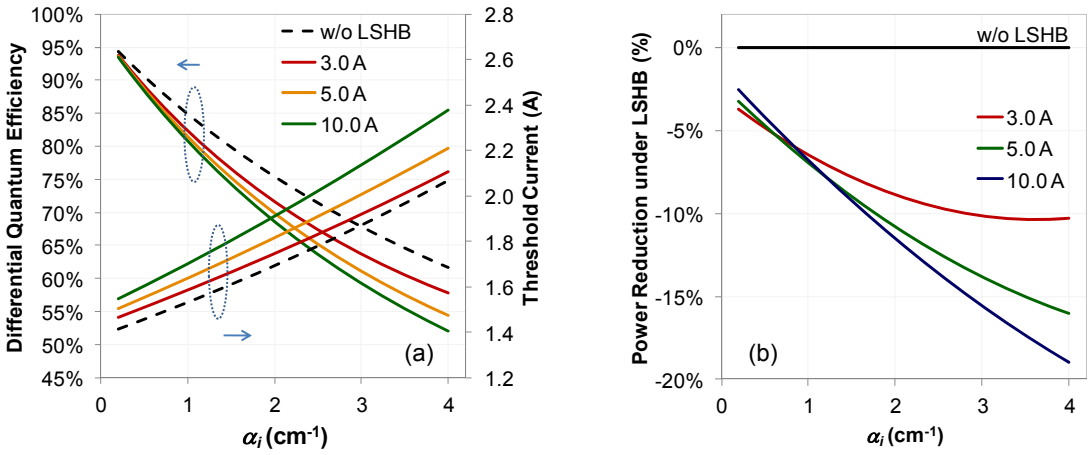

Figure 5. (a) Calculated DQE and threshold current as a function of intrinsic optical loss. (b) Percentage power reduction due to LSHB effect, compared with the case of no LSHB. Thermal effect is not considered.

4. LSHB MITIGATION FOR POWER IMPROVEMENT

In the previous section, LSHB effect is shown to limit power and efficiency of high-power diode lasers. Such impact can be mitigated or even totally compensated through tapered waveguide or longitudinal patterning of electrical contact, therefore enhancing the power and efficiency of high-power diode lasers. For example, laser diode with longitudinally flared waveguide was fabricated to reduce the longitudinal inhomogeneity of the optical field and consequently reduce the LSHB effect [7,8]. An alternative approach is to pattern electrical contact longitudinally (non-uniform current injection) without affecting the lateral gain or optical modal distribution. Both of these approaches are studied theoretically as follow.

One of our proposed approaches for mitigating LSHB is through tapered waveguide design, which is to reduce the longitudinal photon density inhomogeneity. A gradually increasing lateral waveguide width towards the PR facet is used to expand the optical mode to compensate the normally near-exponential increase of photon density, therefore reducing the gain saturation in the device. Figure 6(a) shows several profiles of such tapered waveguide designs, compared with a straight waveguide. Different from the designs demonstrated in [7,8], we set the areas of the tapered waveguides to be the same as that of the straight waveguide, which, in this case, has a 150 μm stripe width for nLIGHT's 1470 nm diode lasers. This is to maintain the same threshold current for the different designs, as well as maintaining similar thermal resistance (to the first order), so that thermal performance differences between devices can be ruled out as origin for power performance enhancement. Using the previously described phenomenological model that incorporates LSHB, we simulate the 1470 nm diode lasers under the several taper profiles shown in Figure 6(a). Both the photon and carrier density inhomogeneity, displayed in Figure 6(b) and (c), are calculated to be reduced for all the taper profiles compared with those of the straight waveguide, with the inhomogeneity almost completely compensated in profile 2. Optical power and efficiency of the several tapered designs are also calculated and compared with the straight waveguide in Figure 6(d). Performance in all three tapered designs is shown to be greatly improved from the straight waveguide. Specifically, a 17% improvement of the optical power is predicted for the 1470 nm laser diodes at an operating current of 10 A, with the most power and efficiency improvement from the most asymmetric tapered structure.

An alternative approach is to pattern the electrical contact longitudinally to mitigate or compensate the LSHB effect. A higher current density is injected, through patterned contact, on the PR side than that on the HR side. This is shown from the carrier density rate equation of Eq. (1) to provide extra injected carrier to compensate gain saturation caused by the normally high photon density near the PR side. The contact patterning approach does not modify the lateral gain or optical modal distribution, therefore avoiding possible reduction of laser brightness due to widened front-facet

waveguide width and likely performance degradation due to increased scattering loss in the taper structure. Design and device implementation are currently in progress.

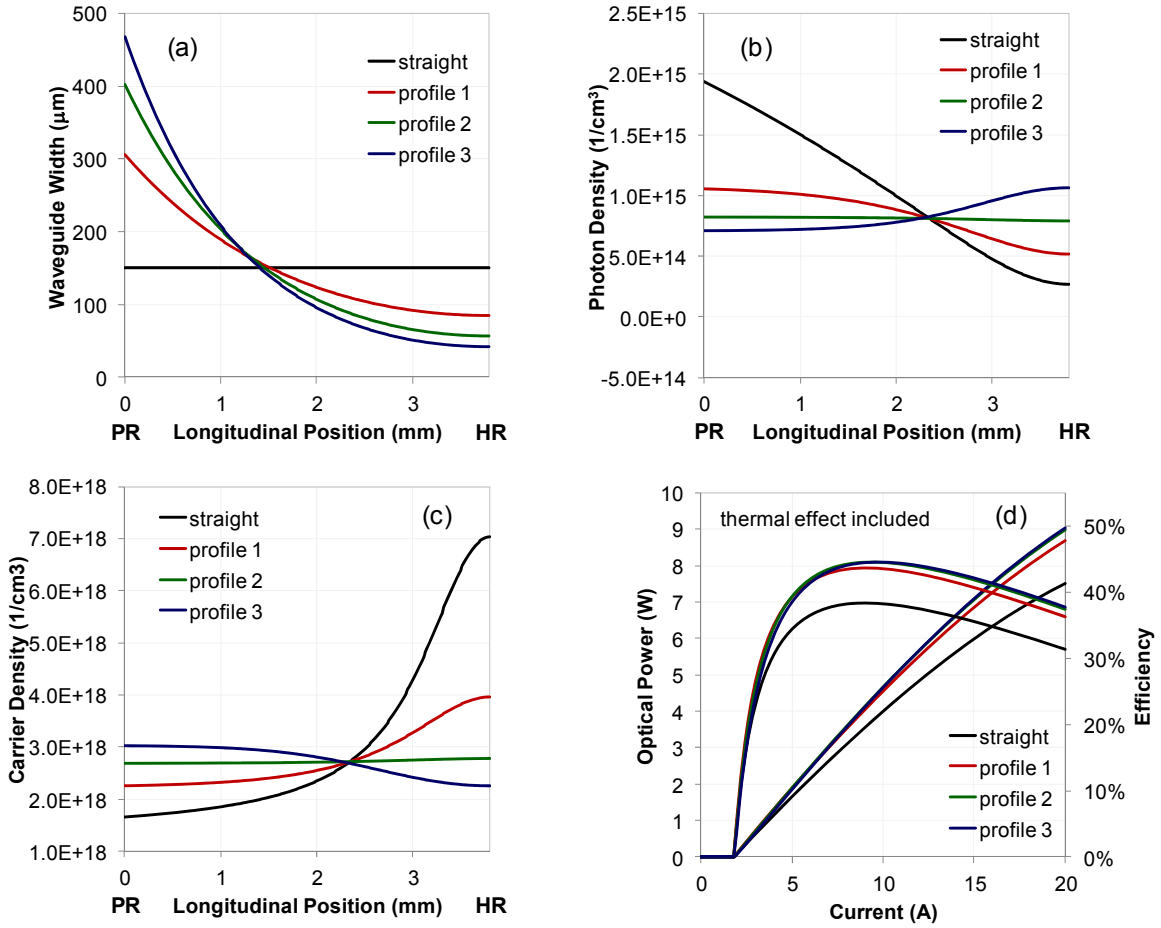

Figure 6. (a) Several tapered waveguide profiles used in the simulation, compared with a straight waveguide. (b) and (c) Calculated photon and carrier density distributions for the taper profiles and straight waveguide, respectively. (d) Calculated L-I characteristics and conversion efficiency for the taper profiles and straight waveguide. Thermal effect is included.

5. CONCLUSION

In conclusion, we present a phenomenological model that incorporates LSHB to describe longitudinal density inhomogeneity in laser diodes. The impact of LSHB on the power efficiency is discussed through numerical calculation, and can be significant under high power operations, and in devices with high intrinsic optical loss. This presents new guidelines for high-power diode laser designs, in which LSHB imposes limits on reducing facet reflectivity and/or increasing cavity length. To achieve high power and high efficiency in laser diodes, effects from LSHB needs to be mitigated, through tapered waveguide and/or longitudinal contact patterning. As an example, an optical power improvement of 17% is predicted for nLIGHT's 1470 nm laser diodes when LSHB effect is compensated.

REFERENCES

[1] Hasuo, S. and Ohmi, T., "Spatial Distribution of the Light Intensity in the Injection Lasers," Jap. J. Appl. Phys. 13, 1429-1434 (1974).

[2] Fang, W-C., *et al.*, "Longitudinal spatial inhomogeneities in high-power semiconductor lasers," IEEE J. Sel. Topics Quantum Electron. 1, 117-128 (1995).

[3] Rinner, F., *et. al.*, "Longitudinal carrier density measurement of high power broad area laser diodes," Appl. Phys. Lett. 80, 19-21 (2002).

[4] Wang, X., *et. al.*, "Root-Cause Analysis of Peak Power Saturation in Pulse-Pumped 1100 nm Broad Area Single Emitter Diode Lasers," IEEE J. Quantum Electron. 46, 658-665 (2010).

[5] Wenzel, H. *et. al.*, "Theoretical and experimental investigations of the limits to the maximum output power of laser diodes," New J. Phys. 12, 1-11 (2010).

[6] Ryvkin, B. S. and Avrutin, E. A., "Spatial hole burning in high-power edge-emitting lasers: A simple analytical model and the effect on laser performance," J. Appl. Phys. 109, 043101 (2011).

[7] Guermache, A., *et. al.*, "Experimental demonstration of spatial hole burning reduction leading to 1480-nm pump lasers output power improvement," IEEE Photon. Technol. Lett. 17 2023-2025 (2005).

[8] Guermache, A., *et. al.*, "New design rules and experimental study of slightly flared 1480-nm pump lasers," IEEE Photon. Technol. Lett. 18 782-784 (2006).

[9] Coldren, L. A. and Corzine, S. W., [Diode Lasers and Photonic Integrated Circuits], Wiley, New York (1995).